Conductance of a single electron transistor with a retarded dielectric layer in the gate capacitor

O. G. Udalov,[1,2] N. M. Chtchelkatchev,[3,4,5] S. A. Fedorov,[4] and I. S. Beloborodov[1]

[1]*Department of Physics and Astronomy, California State University Northridge, Northridge, California 91330, USA*

[2]*Institute for Physics of Microstructures, Russian Academy of Science, Nizhny Novgorod, 603950, Russia*

[3]*L.D. Landau Institute for Theoretical Physics, Russian Academy of Sciences,117940 Moscow, Russia*

[4]*Department of Theoretical Physics, Moscow Institute of Physics and Technology, Moscow 141700, Russia*

[5]*Institute for High Pressure Physics, Russian Academy of Science, Troitsk 142190, Russia*

We study the conductance of a single electron transistor (SET) with a ferroelectric (or dielectric) layer placed in the gate capacitor. We assume that the ferroelectric (FE) has a retarded response with arbitrary relaxation time. We show that in the case of "fast" but still retarded response of the FE (dielectric) layer an additional contribution to the Coulomb blockade effect appears leading to the suppression of the SET conductance. We take into account fluctuations of the FE (dielectric) polarization using Monte Carlo simulations. For "fast" FE, these fluctuations partially suppress the additional Coulomb blockade effect. Using Monte Carlo simulations, we study the transition from "fast" to "slow" FE. For high temperatures, the peak value of the SET conductance is almost independent of the FE relaxation time. For temperatures close to the FE Curie temperature, the conductance peak value nonmonotonically depends on the FE relaxation time. A maximum appears when the FE relaxation time is of the order of the SET discharging time. Below the Curie point the conductance peak value decreases with increasing the FE relaxation time. The conductance shows the hysteresis behavior for any FE relaxation time at temperatures below the FE transition point. We show that conductance hysteresis is robust against FE internal fluctuations.

I. INTRODUCTION

Single electron devices such as single electron transistors (SET), single-electron (and Cooper pair) boxes, chains of metallic islands, etc., are currently in the focus of scientific interest due to their deep and complex physics and numerous promising applications [1–10]. One of the most interesting aspects of these systems is their dynamics. Due to charge quantization, even dc current in a metallic chain of islands leads to a complicated dynamics and to the appearance of voltage oscillations similar to those existing in Josephson junctions [11,12]. The great progress in the fabrication of nanoscale metallic circuits allows the creation of single electron devices coupled to nanomechanical resonators. In addition, SETs with moving metallic islands exist. In these systems, the electrical and mechanical degrees of freedom are coupled leading to a complex dynamics of the whole device. An SET with a mobile metal particle shows the "shuttling" effect [13–17]. Numerous groups studied SET with mobile gate electrodes, which have their own dynamics [10,18–22]. Even a weak electromechanical coupling strongly influences the SET conductance, which is promising for a very sensitive mechanical sensor. A strong electromechanical coupling causes bistability and hysteresis effects, which are useful for memory applications.

Recently, an SET coupled to a ferroelectric (FE) layer was proposed and studied [23,24]. The FE layer can be placed either in the leads-island capacitors or in the gate capacitor. SETs show a high sensitivity of conductivity to the FE dielectric properties. This allows us to consider SETs as an effective way to study the properties of nanosized FE materials. FE hysteresis in combination with its dynamics suggests that a "turnstile" effect should exist in an SET with an FE. This effect is the basis for a precise current standard [25].

When an FE layer is placed in the tunneling junctions, it serves as tunnel barriers for electrons, but the polarization of the FE layers has its own dynamics in contrast to the usual SET where the insulator polarization follows the electric field in the capacitors.

An FE placed in the gate capacitor of an SET [see Fig. 1(a) also has its own dynamics. In this case, the SET has much in common with an SET having a mobile gate where the movement of the electrode causes a change of the gate induced charge. Variations of the FE polarization influence the SET in a similar way. However, there are several important differences between these two systems. Nanomechanical resonators are usually studied as linear oscillators. In contrast, the FE layer shows a nonlinear response since the electric fields in the SET capacitors can exceed the FE saturation field [23,24]. Another important difference is related to the fact that the characteristic time scales of FE materials can be essentially lower than those of the nanomechanical systems and can be even comparable with the characteristic times of the SET. These characteristic time scales of the FE layer and the SET determine the transport properties of the whole system.

Different kinds of FE materials show different dynamics. Shift-type FEs are described by a second-order (in time) differential equation [26]. These materials behave similar to oscillators with a certain resonant frequency ω_0^{FE} (in the linear regime) and a damping time t_{FE}. Order-disorder-type FEs obey the first-order differential equation. These materials are described by the damping time t_{FE} only.

The shortest time scale for SET is $t_c \sim \hbar/E_c$, where E_c is the charging energy. For a metallic grain of few nanometers, this time is of order 10^{-14} s. An intermediate time scale is the electron lifetime on the grain (grain discharging time), $t_d \sim R C_\Sigma$, where R and C_Σ are the resistance and the total
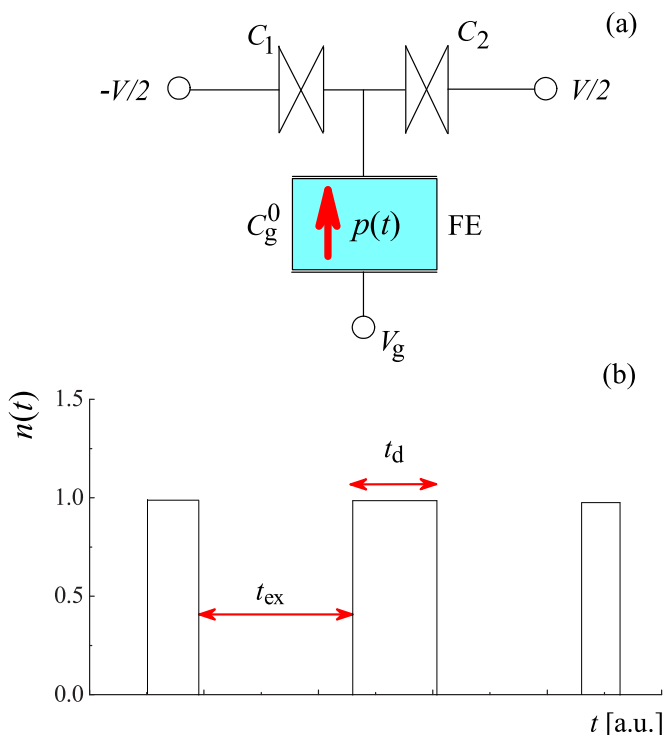
FIG. 1. (Color online) (a) Circuit diagram of SET coupled to **a** FE layer. $C_{1,2}$ are the tunnel junctions capacitance, C_g^0 is the geometrical gate capacitance, $p(t)$ is the time-dependent polarization of the FE layer inside the gate capacitor, V and V_g are the bias and the gate voltages, respectively. (b) Number of excess electrons on the SET metal island n vs time t. SET has the following characteristic times: the electron lifetime on the island (grain discharging time) t_d and the excitation time t_{ex}.

capacitance of the system, respectively. This time depends on the geometry of the system and usually is in the range 10^{-12}–10^{-8} s. The longest time t_{ex} is the time between electron jumps to the grain. In general, this time depends on the gate voltage. For strong Coulomb blockade, it is exponentially large, $t_{ex} \sim R\, C_\Sigma\, e^{E_c/T}$, while for weak Coulomb blockade, due to applied gate voltage, it is comparable to the electron lifetime on the grain, t_d.

The limit, $t_{FE} \ll t_c$, corresponds to the "classical" theory of SET. In this case, the polarization of insulators follows the electric field in the SET capacitors. When the grain charge changes from n to $n \pm 1$ it is implicitly assumed that the polarization of insulators instantly changes from some equilibrium value $p^{eq}|_n$ to a different equilibrium value $p^{eq}|_{n\pm1}$. Thus the "classical" theory of SET considers transitions between states $(n, p^{eq}|_n)$ and $(n \pm 1, p^{eq}|_{n\pm1})$.

The limit, $t_{FE} \gg t_{ex}$, was studied in Refs. [23,24] using the mean-field theory. In this case, the polarization of the FE layers "feels" only the average electric field produced in the SET capacitors. The coupling of an SET with a slow dynamical system causes hysteresis phenomena even in the absence of FE polarization hysteresis. In Ref. [27], an SET with a "slow" dielectric in the gate capacitor was considered.

The region in between the limits discussed above can be divided into three subregions with the following boundaries: (1) $t_{FE} \approx t_c$, (2) $t_{FE} \approx t_d$, and (3) $t_{FE} \approx t_{ex}$. The first region

requires consideration of a single tunneling event by taking into account the time dispersion of the dielectric response. This case is beyond the orthodox theory. Next, two regimes can be treated within the orthodox theory if the polarization time dynamics is taken into account. In the present paper, we consider an SET with a dielectric or an FE layer inside the gate capacitor with relaxation time larger than t_c ($t_{FE} \gg t_c$) but with an arbitrary ratio of t_{FE} and $t_{d,ex}$.

Two different methods are usually used to study the dynamical effects in an SET. The first approach calculates the probabilities of all possible states of the system using a master equation [19,28]. These probabilities are time-dependent in general. This method is mostly used for the investigation of SETs coupled to a mechanical nanoresonator or with a mobile metal island. The mechanical subsystem can be treated classically [15,17,18,21,22] or quantum mechanically [14,16,20,29,30]. The second approach simulates the time evolution of the whole system directly using the Monte Carlo method [11,31]. This approach provides a complete information about the SET behavior and allows us to analyze the time evolution of the system parameters. Currently, single electron counting is possible and the time dependence of the metal island charge can be extracted from the experiment [32]. Therefore the results of Monte Carlo simulations can be compared to real experimental data.

In the present paper, we use Monte Carlo simulations along with analytical consideration to study an SET coupled to a FE layer behaving classically. In particular, we study the influence of the retarded response of the FE layer in the gate capacitor on the Coulomb blockade effects.

The paper is organized as follows. In Sec. II, we describe the model of an SET with an FE (dielectric) layer in the gate capacitor. In Sec. III, we discuss our results: we consider analytically and numerically the SET conductance in the intermediate region $t_c \ll t_{FE} \ll t_d$. We discuss the evolution of the SET conductance with increasing FE relaxation time from $t_{FE} \ll t_d$ to $t_{FE} \gg t_{ex}$. We investigate the influence of the FE (dielectric) internal noise on the SET conductance.

II. MODEL

We consider the SET shown in Fig. 1(a). Left and right electrodes (source and drain) are connected to a metallic island via tunnel junctions. The source and the drain are biased with voltage $\pm V/2$. For simplicity, we assume that all junctions have the same capacitances $C_1 = C_2 = C/2$ and resistances $R_1 = R_2 = R$. An insulator with an instant response is placed inside the tunnel junctions. The polarization of the insulator instantly reacts to the electric field, $p_{1,2} = \chi_{jun}(\pm V/2 - \phi)/d$, where ϕ is the grain potential, d is the junctions thickness, and χ_{jun} is the dielectric susceptibility of the insulator in the junctions. The polarizability of the tunnel barriers is incorporated into capacitances $C_{1,2}$. A gate electrode is capacitively coupled to the metallic island. A voltage V_g is applied to the electrode. An FE (dielectric) with a retarded response is placed between the island and the gate. The characteristic time scale of the material, t_{FE}, is larger than t_c. We assume that the polarization $p(t)$ of the FE (dielectric) layer in the gate capacitor is uniform and time dependent. We use the notation $C_g^0 = S_g / (4\pi d_g)$ for the geometrical capacitance of

the gate-island capacitor, where S_g and d_g are the gate capacitor area and thickness, respectively.

Below, we will distinguish two different temperatures: (1) T_{FE} is the FE layer temperature and (2) T_e is the leads and the island temperature. In general, these temperatures can be different on one hand due to the current flowing through the source-island-drain circuit, which heats the island and the leads [33–35] and on the other hand different temperatures can be created artificially using local heating/cooling techniques [36–39].

A. Free energy of an SET with an FE (dielectric) layer in the gate capacitor

The equations governing the behavior of an SET with an FE (dielectric) layer can be derived using the free energy of the system. The free energy increment can be expressed via the charges q_i and the potentials ϕ_i of all the metallic electrodes $\delta F = \delta R = \sum \phi_i \delta q_i$. Here, the charges are considered as independent variables. In an SET, the three metallic electrodes are biased with a voltage source and the island potential should be found self-consistently. Following the standard approach [40], we introduce a thermodynamic potential where the island charge, the potentials of the leads and the gate potential are considered as independent variables $\delta F_m = \delta F - \delta(V_g Q_g) - \delta(V_1 q_1) - \delta(V_2 q_2) = \phi \delta q - Q_g \delta V_g - q_1 \delta V_1 - q_2 \delta V_2$, where Q_g is the charge of the gate electrode, $q_{1,2}$ and $V_{1,2}$ are the charges and the potentials of the leads, and q and ϕ are the metal island charge and potential, respectively. Below, we use the notation F_m for free energy.

At zero-bias voltage, the increment of this mixed thermodynamic potential has the form $\delta F_m = \phi \delta q - Q_g \delta V_g$. Integration of δF_m over the δq and δV_g provides the total free energy. Using electrostatic considerations for the charge at the gate electrode, we find $Q_g = (C C_g^0 V_g - q C_g^0 - p S_g C)/C_\Sigma$, where $C_\Sigma = C + C_g^0$ is the total capacitance of the system. The grain potential is given by $\phi = (C_g^0 V_g + q - p S_g)/C_\Sigma$. Thus

$$F_m = F_0 + \frac{q^2}{2 C_\Sigma} + \frac{q C_g^0 V_g}{C_\Sigma} - \frac{p S_g q}{C_\Sigma} + \frac{p S_g C V_g}{C_\Sigma} - \frac{C C_g^0 V_g^2}{2 C_\Sigma},$$

(1)

where F_0 is the system free energy at zero gate voltage and zero grain charge:

$$F_0 = (\alpha_P p^2/2 + \beta_P p^4/4 + p^2 S_g/(2 C_\Sigma d_g)) S_g d_g.$$

(2)

The first two terms in Eq. (2) are the usual contributions to the free energy describing the dielectric materials and FEs close to the paraelectric-ferroelectric phase transition [26]. Here α_P and β_P are the phenomenological constants. For dielectric materials both constants are positive. For FEs, the constant α_P linearly depends on the temperature and crosses zero at the FE phase transition point. The last term in Eq. (2) is due to the nonzero electric field $E_0 = -4\pi C_g^0 p/C_\Sigma$ acting on the FE layer at $q = 0$ and $V_g = 0$.

At finite bias voltage V, the free energy F_m needs to be modified: F_m gets an additional contribution $\pm eV/2$ when an electron is added to the grain.

From the linear instant relation between the polarization p and the electric field, $p(t) = \chi_0^i (\phi(t) - V_g)/d_g$, we obtain the free energy of the SET with the properly renormalized capacitances $C_g = C_g^0 \epsilon_0$ and $\tilde{C}_\Sigma = C + C_g$, where $\epsilon_0 = 1 + 4\pi \chi_0^i$ is the effective dielectric constant of the layer in the gate capacitor.

B. Ferroelectric dynamics

Varying the free energy in Eq. (1) with respect to the polarization p, we find the equation governing p. Below, we consider FEs (dielectrics) of the order-disorder type. These materials are described using the first-order time-dependent equation [26]

$$\gamma \dot{p} = -\frac{\partial F_m}{\partial p} + \tilde{\Gamma}_L,$$

(3)

where γ is the relaxation constant related to the relaxation time, $t_{FE} = \gamma \chi_0$, with $\chi_0 = \alpha_P^{-1}$ being the linear response of the polarization to the external electric field. $\tilde{\Gamma}_L$ describes an intrinsic noise of the FE layer. Substituting the free energy F_m into Eq. (3) we obtain the following nonlinear equation for the polarization:

$$\gamma \dot{p} + \alpha_P p + \beta_P p^3 = \frac{q - C V_g - p S_g}{C_\Sigma d_g} + \tilde{\Gamma}_L.$$

(4)

We introduce the paraelectric-ferroelectric Curie temperature at which the coefficient in front of the linear term is zero, $\chi^{-1} = \alpha_P + 4\pi C_g^0/C_\Sigma = \tilde{\alpha}_P(T_{FE} - T_C) = 0$. We call the material inside the gate capacitor as a FE material if the Curie temperature is positive $T_C > 0$. For $T_{FE} > T_C$, Eq. (4) has only one solution, while for $T_{FE} < T_C$ the spontaneous polarization appears leading to multiple solutions of the equation.

Another Curie temperature T_C^0 can be introduced using the relation $\chi_0^{-1} = \tilde{\alpha}_P^0(T_{FE} - T_C^0) = 0$. It corresponds to the same FE but confined by the shorted metal electrodes. One can see that $T_C < T_C^0$. When an FE is placed in between the shorted metal electrodes, the potential difference and the electric field are fixed across the FE layer. In contrast, in the SET problem, the potential of the metal island should be found self-consistently. Therefore the equation governing the FE layer gives the lower Curie temperature. Physically, this reflects the fact that the depolarizing electric field inside the FE layer is not fully screened by the metal island in the SET. This complicates the appearance of the spontaneous polarization.

We notice that χ_0 is the susceptibility of the FE (dielectric) layer with respect to the external electric field, while χ is the susceptibility with respect to the external charges q and $Q_0 = -C_g^0 V_g$. Below, we will refer to Q_0 as the gate charge. However, Q_0 is not the real charge at the gate electrode and it differs from Q_g which was introduced above. For $T_{FE} > T_C$, two susceptibilities χ and χ_0 are related as follows $\chi^{-1} = \chi_0^{-1} + 4\pi C_g^0/C_\Sigma$. For FE (dielectric) materials with instant response, the constant χ_0 defines the dielectric permittivity, $\chi_0^i = \chi_0$ and $\epsilon_0 = 1 + 4\pi \chi_0$.

We regard the material in the gate capacitor as a dielectric if the quantity, $\alpha_P + 4\pi C_g^0/C_\Sigma > 0$, is positive for any temperature. In general, we can consider the dielectric material as the material with the negative Curie temperature, $T_C < 0$.

In our Monte Carlo simulations, we solve the nonlinear Eq. (4) directly. For analytical consideration at temperatures $T_{FE} > T_C^0$, we linearize Eq. (4):

$$\gamma \dot{q}_p + \chi^{-1} q_p = \frac{4\pi C_g^0 (q - C V_g)}{C_\Sigma} + \Gamma_L. \qquad (5)$$

Here, we introduce the charge $q_p = p S_g$ and $\Gamma_L = S_g \tilde{\Gamma}_L$.

We mention that below T_C^0 the susceptibility χ_0 becomes negative. However, the FE layer is still in the paraelectric phase for temperatures $T_C < T_{FE} < T_C^0$. We show that in this temperature region Eq. (5) is not valid since it produces divergent solutions for q_p and q. The nonlinear term $\beta_P p^3$ should be taken into account to restrict variations of q_p and q.

C. Langevin forces

Internal fluctuations of the FE layer occur due to the interaction of FE (dielectric) polarization with all other degrees of freedom in the FE layer. This interaction has two components. The "regular" component leads to the appearance of polarization relaxation. This term can be written in the form $\gamma \dot{q}_p$ even for nonlinear systems [41]. Another noise component is responsible for fluctuations of the FE layer polarization. It appears in the RHS of Eq. (4) as a random Langevin force $\tilde{\Gamma}_L$. If the polarization varies slowly in time in comparison to the characteristic time of internal FE processes the correlation function of the Langevin forces can be chosen as $C_L = \langle \tilde{\Gamma}_L(t) \tilde{\Gamma}_L(t') \rangle = 2\gamma k_B T_{FE} \delta(t - t')/(S_g d_g)$. The relation between the relaxation constant γ and the Langevin forces dispersion is valid even for nonlinear systems [41]. The dispersion of the polarization fluctuations in the linear response regime ($\beta_P \ll \alpha_P p^2$) can be written using the FE layer susceptibility as follows $D_p = \langle (\Delta p)^2 \rangle = \chi k_B T_{FE}/(S_g d_g)$. Below, we will use this expression for estimates. For strong nonlinear effects ($\beta_P \sim \alpha_P p^2$), the polarization dispersion is given by a more complicated expression [42].

D. SET dynamics

The probability of electron hop to/from the metallic island is given by the expression

$$G_{1,2}^\pm = \frac{1}{e^2 R} \frac{\Delta F_{1,2}^\pm}{e^{\Delta F_{1,2}^\pm / T_e} - 1}, \qquad (6)$$

where

$$\Delta F_1^\pm = 2 E_c \left(\pm \left(n + \frac{C_g^0 V_g}{e} + \frac{C_\Sigma V}{2e} - \frac{q_p}{e} \right) + 1/2 \right),$$
$$\Delta F_2^\pm = 2 E_c \left(\pm \left(n + \frac{C_g^0 V_g}{e} - \frac{C_\Sigma V}{2e} - \frac{q_p}{e} \right) + 1/2 \right). \qquad (7)$$

Subscript (1,2) denotes the electrode from which (or to which) an electron jumps. Superscript $+$ describes electron hopping from a certain lead to the particle. Superscript "$-$" describes electron hopping from the island to a certain lead. $n = q/e$ is the island population. $E_c = e^2/(2 C_\Sigma)$ is the bare charging energy.

An important assumption made when we calculate ΔF is that the polarization p does not change during the electron hop since $t_{FE} \gg t_c$. Equation (7) describes the processes

$(n, p(t)) \rightarrow (n \pm 1, p(t))$. This is in contrast to the "classical" SET situation where the polarization p adjusts during the hop and the following processes occur: $(n, p^{eq}|_n) \rightarrow (n \pm 1, p^{eq}|_{n\pm1})$.

Two characteristic times can be introduced using Eq. (6): (1) the excitation time t_{ex} corresponding to the island charging event at zero gate voltage, $V_g = 0$ (this event is suppressed due to the Coulomb blockade effect, $t_{ex} = G_1^+|_{n=0,V_g=0,q_p=0,V=0} \sim R C_\Sigma e^{E_c/T_e}$); and (2) the relaxation time t_d, which corresponds to the discharging of the charged island. This time is much shorter, $t_{ex} \gg t_d$, since there is no exponential factor in this case, $t_d = G_1^-|_{n=1,V_g=0,q_p=0,V=0} \sim R C_\Sigma$. We mention that excitation time depends strongly on the gate voltage V_g and for certain voltages both times are comparable.

The island population is defined by the random electron jumps from and to the island:

$$\dot{n}(t) = \sum_i Z_i \delta(t - t_i). \qquad (8)$$

Here, Z_i has three possible values ± 1 and 0. The probability for an electron to hop per unit time is defined by Eq. (6). It depends on the bias voltage V, the gate voltage V_g, the number of electrons on the island $n(t)$, and the FE layer induced charge $q_p(t)$. The last two quantities depend on the time leading to time dependent hopping probabilities. Thus one has to solve self-consistent equations for the FE layer and the SET.

We use numerical Monte Carlo simulations [11] to solve coupled SET and FE equations. Equation (8) can be written in the discrete form

$$n(t_i) = n(t_{i-1}) + Z(n(t_{i-1}), q_p(t_{i-1})) dt,$$
$$Z = \begin{cases} 1, x < G_1^+ + G_2^+, \\ 0, G_1^+ + G_2^+ < x < 1 - (G_1^- + G_2^-), \\ -1, x > 1 - (G_1^- + G_2^-), \end{cases} \qquad (9)$$

where x is the random value uniformly distributed between 0 and 1, $dt = t_i - t_{i-1}$. The time interval dt is much shorter than all characteristic times in the problem, $dt \ll t_d, t_{FE}$.

The average electric current through the SET can be calculated as follows:

$$I = \frac{e}{T_m} \sum_i \zeta(t_i),$$
$$\zeta = \begin{cases} 1, Z(t_i) > 0 \wedge y < G_1^+/(G_1^+ + G_2^+), \\ -1, Z(t_i) < 0 \wedge y < G_1^-/(G_1^- + G_2^-), \\ 0, Z(t_i) = 0, \end{cases} \qquad (10)$$

where y is the random number uniformly distributed between 0 and 1; T_m is the measurement time interval.

III. CONDUCTANCE OF SET WITH RETARDED FE (DIELECTRIC) LAYER

We investigate the behavior of the SET conductance as a function of the gate voltage V_g for different ratios of the FE (dielectric) relaxation time t_{FE} and SET characteristic times t_{ex} and t_d.

A. Suppression of Coulomb blockade due to internal noise of FE

The conductance peaks as a function of the gate charge Q_0 have a finite width at finite temperatures. The width of these peaks is defined as $\Delta Q_0^{\mathrm{L}} \approx e k_{\mathrm{B}} T_{\mathrm{e}} / E_{\mathrm{c}}$. The polarization of the FE (dielectric) layer enters the SET equations as an additional gate capacitor charge. Therefore the FE (dielectric) polarization fluctuations can be considered as fluctuations of the gate charge Q_0. These fluctuations average the SET conductance over the region $\Delta Q_0^{\mathrm{p}} \sim \sqrt{D_{\mathrm{p}}} \sim \sqrt{T_{\mathrm{FE}}}$. Due to the square root dependence of ΔQ_0^{p} on temperature, the internal fluctuations of the FE polarization produce much stronger effect on the conductance than the finite temperature of the leads. If the temperature of the FE layer T_{FE} equals to the source and drain electrodes temperatures, T_{e}, then the FE fluctuations are negligible for temperatures $k_{\mathrm{B}} T_{\mathrm{FE}} \ll 2\pi \chi C_{\mathrm{g}}^0 E_{\mathrm{c}} / C_\Sigma$. Also, FE fluctuations can be neglected for temperatures, $T_{\mathrm{FE}} \ll T_{\mathrm{e}}$.

If ΔQ_0^{p} exceeds the half of an electron charge, the Coulomb blockade effect is smeared and the conductance peaks as a function of the gate voltage disappear. Thus the general condition for observation of charge quantization effects relates the polarization dispersion and the electron charge, $S_{\mathrm{g}} \sqrt{D_{\mathrm{p}}} \ll e/2$. Below, we show that FE fluctuations can increase the SET conductance in some cases.

B. SET with "instant" FE (dielectric) in the gate capacitor

We call FEs (dielectrics) with $t_{\mathrm{FE}} \ll t_{\mathrm{c}}$ as FEs (dielectrics) with instant response, for brevity, we call them "instant" FEs (dielectrics). In contrast, we call FEs "retarded" if $t_{\mathrm{FE}} \gg t_{\mathrm{c}}$. An SET with "instant" dielectrics was studied in many papers using the orthodox theory. In this case the conductance is a periodic function of the gate charge Q_0. The conductance maxima are located at points $Q_0 = e(l + 1/2)/\epsilon_0$, where l is an integer number. The peak value of the SET conductance in this case is $\sigma_0 = 1/(4R)$. The conductance is suppressed between peaks due to the Coulomb blockade effect.

If an SET is coupled to an FE with a relaxation time $t_{\mathrm{FE}} \approx t_{\mathrm{c}}$, the SET can not be studied within the orthodox theory. This case requires the calculation of tunneling matrix elements of electrons interacting with the FE (dielectric) polarization, which varies on time scale t_{c}. Tunneling in the presence of time dispersion was considered in the past [43–45]. It was shown that time dispersion, caused by the dissipation in the tunnel junction circuit, leads to the decrease of the junction conductance and to the appearance of an effective Coulomb blockade effect.

C. SET with "fast" FE (dielectric) in the gate capacitor ($t_{\mathrm{FE}} \ll t_{\mathrm{d}}$)

In the case of "fast" FE (dielectric), $t_{\mathrm{c}} \ll t_{\mathrm{FE}} \ll t_{\mathrm{d}}$, each electron jump to the grain or out of grain occurs when the polarization is in its equilibrium state at a given grain population n. However, during the jump, the FE (dielectric) polarization preserves its value since $t_{\mathrm{FE}} \gg t_{\mathrm{c}}$, meaning that the state of the FE polarization is not at equilibrium after the jump. We define the state of the SET at each moment with the pair $(n(t), p(t))$. The following transitions correspond to the events of grain charging and discharging $(n, p|_n^{\mathrm{eq}}) \to (n \pm 1, p|_n^{\mathrm{eq}})$, where $p|_n^{\mathrm{eq}}$ stands for equilibrium polarization at given

n and Q_0:

$$\chi^{-1} p^{\mathrm{eq}}|_n + \beta_{\mathrm{P}}(p^{\mathrm{eq}}|_n)^3 = \frac{en + C Q_0/C_{\mathrm{g}}^0}{C_\Sigma d_{\mathrm{g}}}. \qquad (11)$$

We mention that for an SET with "instant" insulators, different kind of transitions occur $(n, p|_n^{\mathrm{eq}}) \to (n \pm 1, p|_{n \pm 1}^{\mathrm{eq}})$.

Consider the free energy difference in Eq. (7) as a function of the island population n at $V = 0$. The stable population of the island is approximately defined by the conditions

$$\Delta F^+(n + 1, p^{\mathrm{eq}}|_{n+1}) > \Delta F^-(n + 1, p^{\mathrm{eq}}|_{n+1}),$$
$$\Delta F^+(n, p^{\mathrm{eq}}|_n) < \Delta F^-(n, p^{\mathrm{eq}}|_n). \qquad (12)$$

We find approximately the "equilibrium" value of n and polarization p at a given value of Q_0 using the following equation:

$$\Delta F^+(n^{\mathrm{eq}}, p^{\mathrm{eq}}|_{n^{\mathrm{eq}}}) = \Delta F^-(n^{\mathrm{eq}}, p^{\mathrm{eq}}|_{n^{\mathrm{eq}}}). \qquad (13)$$

Here, n^{eq} stands for approximately the most probable population of the island, it may have a noninteger value. Equation (13) can be rewritten in the form

$$en^{\mathrm{eq}} - Q_0 - q_{\mathrm{p}}^{\mathrm{eq}}|_{n^{\mathrm{eq}}} = 0, \qquad (14)$$

where $q_{\mathrm{p}}^{\mathrm{eq}}|_{n^{\mathrm{eq}}} = S_{\mathrm{g}} p^{\mathrm{eq}}|_{n^{\mathrm{eq}}}$. Using Eq. (11), we can relate the "equilibrium" polarization and the gate charge Q_0:

$$\alpha_{\mathrm{P}}\left(q_{\mathrm{p}}^{\mathrm{eq}}|_{n^{\mathrm{eq}}}\right) + \tilde{\beta}_{\mathrm{P}}\left(q_{\mathrm{p}}^{\mathrm{eq}}|_{n^{\mathrm{eq}}}\right)^3 = 4\pi Q_0, \qquad (15)$$

where $\tilde{\beta}_{\mathrm{P}} = \beta_{\mathrm{P}}/S_{\mathrm{g}}^2$. Equation (15) has a unique solution for temperatures $T_{\mathrm{FE}} > T_{\mathrm{C}}^0$. For $T_{\mathrm{FE}} < T_{\mathrm{C}}^0$, it has three different solutions. Introducing $p^{\mathrm{eq}}|_{n^{\mathrm{eq}}}$ into Eq. (14), we find the "equilibrium" population n^{eq}. At a given Q_0, the whole system state most probably will be in the vicinity of n^{eq}. To find approximately the SET conductance, we take into account only two states n_1 and n_2 ($n_1 < n_2$) nearest to n^{eq}. Using the expression

$$\sigma = \frac{e}{V} \frac{\tilde{G}_2^+ \tilde{G}_1^- - \tilde{G}_1^+ \tilde{G}_1^-}{\tilde{G}_1^+ + \tilde{G}_2^+ + \tilde{G}_1^- + \tilde{G}_2^-}, \qquad (16)$$

we find the SET conductance. We use the following notations in Eq. (16): $\tilde{G}_{1,2}^+ = G_{1,2}^+|_{n=n_1}$, $\tilde{G}_{1,2}^- = G_{1,2}^-|_{n=n_2}$. Below, we consider the behavior of the SET conductance at different temperatures.

1. $T_{\mathrm{FE}} > T_{\mathrm{C}}^0$.

In this temperature region, the parameter α_{P} is positive and Eq. (15) has only one solution leading to one "stable" state for the whole system. Figure 2 shows the free energy difference as a function of the island population n for $C_{\mathrm{g}}^0 = 0.2 C_\Sigma$, $\alpha_{\mathrm{P}} = 1.5$, $e^2 \tilde{\beta}_{\mathrm{P}} = 0.13$, and $Q_0 = 0.5e$. Inequalities (12) are satisfied for $n = 3$ only. Equation (15) gives the "equilibrium" population n^{eq} slightly higher than 3. The most probable states are $n = 3$ and $n = 4$. Figure 3 shows the SET conductance [Eq. (16)] as a function of the gate charge Q_0 for parameters $C_{\mathrm{g}}^0 = 0.005 C_\Sigma$, $\alpha_{\mathrm{P}} = 0.12$, $e^2 \tilde{\beta}_{\mathrm{P}} = 0.0013$, and $T_{\mathrm{e}} = 0.2 E_{\mathrm{c}}$. These parameters correspond to TTF-CA FE at $T_{\mathrm{FE}} = 120$ K [46]. This FE has a rather small relaxation time in the picosecond region [47], which can be comparable, smaller, or larger than the discharging time of the SET. The conductance appears as a series of peaks. The period and
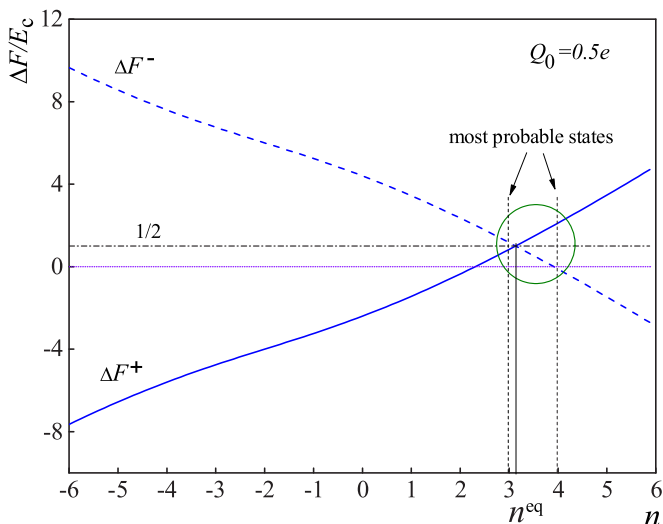
FIG. 2. (Color online) Free energy difference, Eq. (7), at $V = 0$ and $Q_0 = 0.5e$ vs n. The solid line shows $\Delta F^+(n)$, the dashed line shows $\Delta F^-(n)$. Intersection of ΔF^+ and ΔF^- shows the most probable state of the SET at a given Q_0.

the height of the peaks are not constant due to the nonlinear term in Eq. (4). The red circle shows a typical region where Eq. (16) is not valid. In this region, at least three states are involved in the electron transport, whereas Eq. (16) accounts for only two states. The dashed line shows the conductance calculated using numerical Monte Carlo (MC) simulations. We use $\gamma = 0.05 R\, C_\Sigma$. The numerical and analytical results coincide in the vicinity of the conductance peaks, where Eq. (16) works well. Close to the conductance deeps, the numerical result is more accurate since all possible states are taken into account in the simulations.
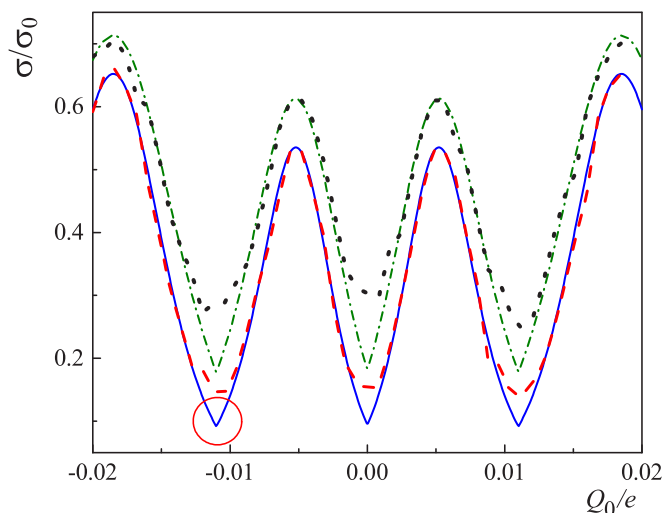

FIG. 3. (Color online) SET conductance vs the gate charge Q_0 for temperatures $T_{\mathrm{FE}} > T_C^0$. The solid blue line is calculated using Eq. (16) at an electron temperature $T_e = 0.2 E_c$. The dashed red line and the dotted black line are obtained using MC simulations. The dashed line is calculated in the absence of FE internal fluctuations. The dotted black line is calculated in the presence of fluctuations. The green dash dotted line is calculated with Eq. (16) at $T_e = 0.26 E_c$. The red circle shows a typical region where Eq. (16) is not valid.

The conductance peaks value is smaller than σ_0 for "fast" FE. Below, we show that this is a consequence of an effective additional Coulomb blockade appearing due to the retarded response of the FE layer.

It is important that Eq. (16) does not take into account the internal fluctuations of the FE polarization. This approximation is valid, for example, for temperatures $T_{\mathrm{FE}} \ll T_e$. To fit the blue curve in Fig. 3 with MC simulations, we turned off the Langevin forces in Eq. (4). The result is the red dashed line.

The dotted black line in Fig. 3 shows the result of the MC modeling for $T_{\mathrm{FE}} = T_e$ in the presence of FE internal fluctuations. One can see that the FE fluctuations are important for electron transport. The internal fluctuations suppress the additional Coulomb blockade increasing the conductance. For comparison, we show the conductance calculated using Eq. (16) for the same SET parameters but with higher electron temperature, $T_e = 0.26\, E_c$ (dash dotted green line).

For a small enough parameter β_{P}, we can neglect nonlinear effects and use the linearized equation for the FE polarization, Eq. (5). In this case, the SET conductance is a periodic function of parameter Q_0 with a period $\Delta Q_0 = e/\epsilon_0$. Consider the conductance in the vicinity of the first peak position $Q_0 = -e/(2\epsilon_0)$. Figure 4 shows different processes contributing to the electron transport of the SET with a "retarded" FE layer. This figure shows a number of branches of the SET free energy as a function of the gate charge Q_0. These branches correspond
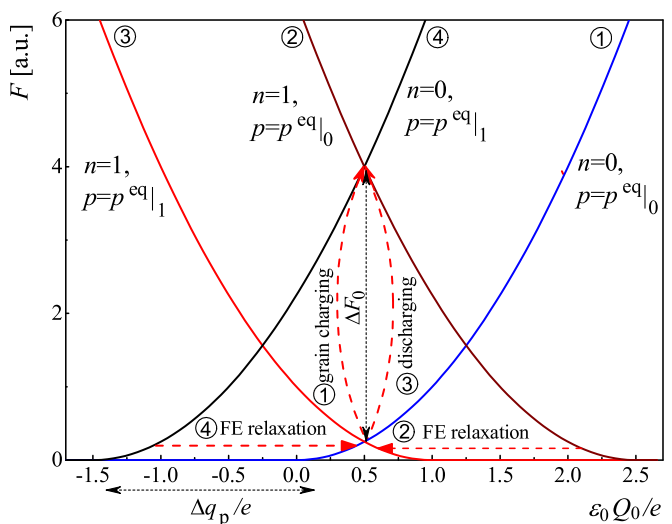

FIG. 4. (Color online) Free energy as a function of gate charge Q_0. Blue branch (1) corresponds to the state $(0, p^{\mathrm{eq}}|_0)$, red branch (3) corresponds to the state $(1, p^{\mathrm{eq}}|_1)$, brown branch (2) shows the free energy for the state $(1, p^{\mathrm{eq}}|_0)$, and black branch (4) shows the state $(0, p^{\mathrm{eq}}|_1)$. At $\epsilon_0 Q_0 = e/2$, in the SET with "instant" insulators, the grain charging and discharging events correspond to the transition from blue to the red branch. The energy gap in this case is zero leading to a large conductance. For an SET with a "retarded" FE, another kind of transitions occur. The island charging event (1) corresponds to the transition from the blue branch (1) to the brown branch (2). After the transition, the FE polarization relaxes to a new equilibrium state [process depicted by the horizontal arrow (2)]. The grain discharging event (3) corresponds to the transition from the red (3) to the black (4) branch. Finally, the FE polarization relaxes again [process (4)]. $\Delta F_0 = 4\pi \chi\, C_g^0 E_c / C_\Sigma,\ \Delta q_{\mathrm{p}} = (4\pi \chi\, C_g^0 / C_\Sigma)e$.

to the island population $n = 0,1$ and the FE polarization $p^{\text{eq}}|_{0,1}$. For an SET with a "retarded" FE, the transitions (charging and discharging events) occur between the states with nonequilibrium polarization of the FE (dielectric) layer. This leads to the appearance of a nonzero energy gap (see Fig. 4) for any gate voltage. Such a gap can be considered as an additional effective Coulomb blockade appearing due to the "retarded" FE (dielectric) response.

At $\epsilon_0 Q_0 = e/2$, the charging event $(0, p|_0^{\text{eq}}) \rightarrow (1, p|_0^{\text{eq}})$ [process (1) in Fig. 4] requires an additional energy $\Delta F_0 = 4\pi \chi C_g^0 E_c / C_\Sigma$. The FE layer relaxes to its equilibrium state $p|_1^{\text{eq}}$ [the process (2) in Fig. 4] after the grain charging event. The discharging process (3) $(1, p|_1^{\text{eq}}) \rightarrow (0, p|_1^{\text{eq}})$ is also inelastic. It requires the same energy ΔF_0. This energy gap suppresses the conductance of the SET with the "retarded" FE layer. For an SET with an "instant" FE (dielectric) layer, the charging and discharging transitions occur directly from branch (1) to branch (3) and do not require any energy at $\epsilon_0 Q_0 = e/2$ leading to a higher conductance.

For temperatures $T_e \ll E_c (4\pi \chi C_g^0 / C_\Sigma)$, the maximum conductance value is

$$\sigma_{\max} \approx \frac{1}{R} \frac{2\pi \chi C_g^0}{C_\Sigma} \frac{E_c}{T_e} e^{-\frac{\Delta F_0}{T_e}}. \qquad (17)$$

The magnitude of the conductance peak increases exponentially with temperature, however, it stays smaller than the "classical" value of the SET conductance σ_0. We mention that for the SETs with "instant" insulators the magnitude of the conductance peak is temperature independent.

2. $T_C < T_{FE} < T_C^0$

In this temperature region, the susceptibility χ_0 is negative and Eq. (15) has three different solutions meaning that there are more than one stable state in the whole SET system. Figure 5
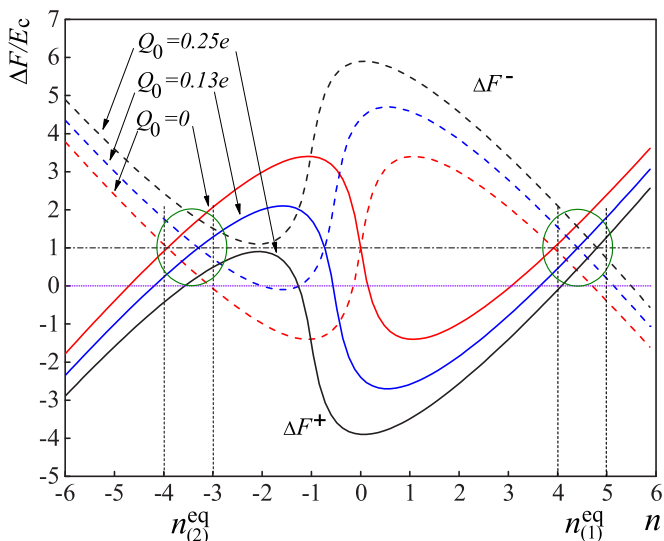

FIG. 5. (Color online) Free energy difference, Eq. (7), at $V = 0$ vs n. Solid lines show $\Delta F^+(n, p^{\text{eq}}|_n)$, dashed lines show $\Delta F^-(n, p^{\text{eq}}|_n)$. Red lines correspond to $Q_0 = 0$, blue lines show $\Delta F^\pm$ at $Q_0 = 0.13e$, and black lines show the case of $Q_0 = 0.25e$. Negative χ_0 provides the negative slope of ΔF^+ and positive slope of ΔF^- in the vicinity of $n = 0$.

shows $\Delta F^\pm(n, p^{\text{eq}}|_n)$ for different Q_0 for the following SET parameters $\alpha_P = -2$, $\chi^{-1} = 0.513$, $e^2 \tilde{\beta}_P = 0.13$, and $C_g^0 = 0.2 C_\Sigma$.

Here the dependencies are nonmonotonic in contrast to the case $T_{FE} > T_C^0$. Consider the blue curves corresponding to $Q_0 = 0.13e$. One can see that the state with zero island population is not stable. Two stable states, shown by the green circles, occur in the vicinity of $n_{(1)}^{\text{eq}} \approx 4.5e$ and $n_{(2)}^{\text{eq}} \approx -3.5e$. Depending on the initial system state both "equilibrium" populations can be realized. In this case, one can expect the hysteresis behavior of the SET conductance as a function of the gate voltage. Figure 5 shows that for high enough gate voltage (black lines) only one stable state remains meaning that conductance hysteresis exists only around $Q_0 = 0$. This is in contrast to the case of SET with "slow" FE considered in Refs. [23,24], where hysteresis appears in the vicinity of each conductance peak. The nature of hysteresis in the case of "slow" FE in the gate capacitor is very different from the case of "fast" FE (dielectric). For "fast" FE the hysteresis is related to the instability ($\chi_0 < 0$) of the FE dielectric properties, while for "slow" FE the hysteresis occurs even in the absence of FE instability due to the interaction of the fast SET system with the slow FE layer.

Note that in the region $T_C < T_{FE} < T_C^0$ the nonlinear term in Eq. (4) for the FE polarization can not be neglected since the population $n(t)$ and the polarization $p(t)$ will be divergent functions.

Figure 6 shows the SET conductance as a function of the gate charge Q_0 for the following parameters: $\alpha_P = -0.12$, $e^2 \tilde{\beta}_P = 0.0013$, and $C_g^0 = 0.02 C_\Sigma$. These parameters correspond to TTF-CA FE at $T_{FE} \approx 50$ K [46]. Solid lines demonstrate the result obtained using Eq. (16) at $T_e = 0.2 E_c$ [panel (a)] and $T_e = 0.3 E_c$ [panel (b)]. One can see that there are two branches of the conductance as a function of the gate voltage. Dashed and dotted lines demonstrate the conductance obtained using MC simulations in the absence of FE internal fluctuations [panel (a)] and in the presence of fluctuations [panel (b)]. To obtain the red dashed lines, we increase Q_0 from $-0.5e$ to $+0.5e$. The initial polarization and the island population at each Q_0 were taken from the last simulation point at previous Q_0. Dotted lines correspond to the case of decreasing Q_0. MC simulations confirm the existence of the conductance hysteresis. The analytical and numerical curves agree well with each over. Part of the conductance branches, for example, between $Q_0 = 0.1e$ and $0.25e$, obtained using Eq. (16) is not realized in numerical simulations within the chosen protocol. To observe these branches, we need to set special initial conditions in our system, which is hard to realize in an experiment.

Panel (b) shows the result of simulations in the presence of FE internal fluctuations ($T_{FE} = T_e$). One can see that fluctuations suppress the Coulomb blockade and increase the conductivity. The peak positions stay the same. The FE fluctuations at given parameters do not smear the hysteresis.

3. $T_{FE} < T_C$

In this region, the solution of Eq. (4) becomes ambiguous leading to a more complicated behavior of the SET. Two different equilibrium polarizations $p_{1,2}^{\text{eq}}|_n$ correspond to a single island population value n. Consider the free energy
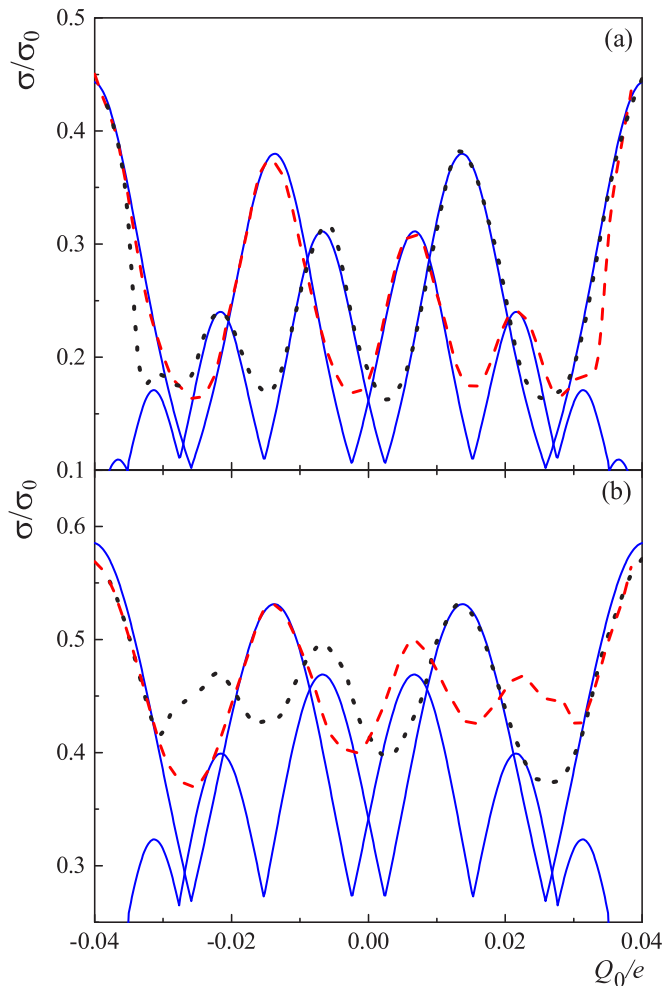
FIG. 6. (Color online) The conductance of an SET as a function of the gate charge Q_0 for temperatures $T_C < T_{FE} < T_C^0$. Solid blue lines are calculated using Eq. (16). In the vicinity of $Q_0 = 0$, there are two branches of the conductance due to the SET instability. The dashed red line and dotted black line are calculated using MC simulations. The dashed line is obtained for an increasing parameter Q_0 during simulations, while the dotted line is obtained for decreasing Q_0. (a) shows results obtained using Eq. (16) at $T_e = 0.2E_c$ and results of MC simulations at $T_e = 0.2E_c$ in the absence of FE internal fluctuations. (b) shows results obtained using Eq. (16) at $T_e = 0.3E_c$ and results of MC simulations in the presence of FE internal fluctuations and at $T_e = 0.2E_c$.
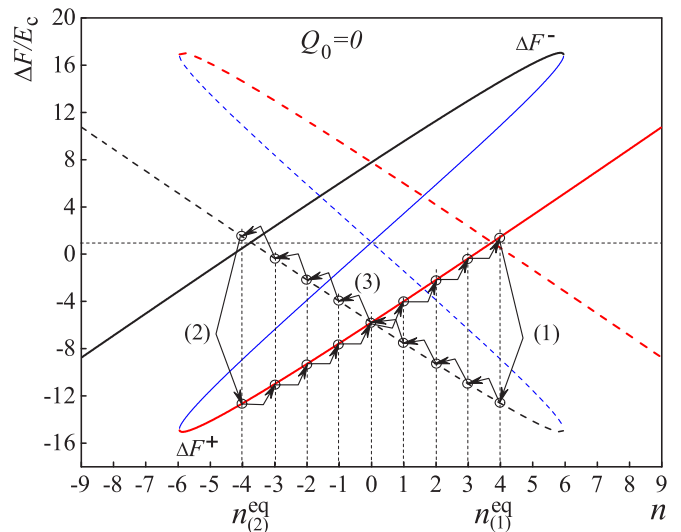

FIG. 7. (Color online) Free energy difference, Eq. (7), at $V = 0$ and $Q_0 = 0$ vs n. Solid lines show $\Delta F^+(n, p_{1,2}^{eq}|_n)$, dashed lines show $\Delta F^-(n, p_{1,2}^{eq}|_n)$. Various colors correspond to different FE layer polarization states. Blue lines show the unstable polarization state, $p_3^{eq}|_n$, which can not be realized in an experiment. Red line stands for positive polarization, black line corresponds to negative polarization. Black arrows show possible behavior of the SET.

difference as a function of n at $\alpha_P = -7$, $e^2\tilde{\beta}_P = 0.5$, $C_g^0 = 0.1\,C_\Sigma$, and $Q_0 = 0$ (Fig. 7). Quantities $\Delta F^\pm$ have two branches depicted by red and black curves. These branches correspond to equilibrium polarization states $p_1^{eq}|_n$ and $p_2^{eq}|_n$. Blue lines show unstable solutions. "Equilibrium" population $n_{(1)}^{eq}$ is defined by the intersection of two red lines. In contrast to the case of $T_{FE} > T_C$, there is an additional allowed state at $n = n_{(1)}^{eq}$ corresponding to another FE polarization. Due to inequalities (12), this second state is unstable with respect to variations of n. The internal fluctuations of the FE polarization may cause switching of the polarization [process (1) in Fig. 7] leading to the transition to another "equilibrium" population state $n_{(2)}^{eq}$. We depict a possible dynamical process in the SET

in Fig. 7 by the black arrows. The system switches back and forth between two population states, $n = n_{(1)}^{eq}$ and $n = n_{(2)}^{eq}$.

The temperature driven transition between two FE equilibrium polarization states is defined by the energy barrier between these two states, which can be estimated as $\Delta W_p \approx 2S_g d_g \alpha_P^2/(\beta_P) = 2\alpha_P^2/(4\pi\tilde{\beta}C_g^0)$. Varying parameters one can make this barrier much higher than E_c, thus prohibiting the polarization switching. In this case, there is no population "wandering" and the whole system behaves similarly to the case of $T_{FE} > T_C$. In particular, the conductance shows hysteresis as a function of Q_0. For parameters used in Fig. 7, $\Delta W_p > 100E_c$. Therefore processes (1) and (2) are almost prohibited. The hysteresis behavior in the system with the above parameters is rather robust.

The hysteresis can also be smeared through the consecutive change of n. The transition between $n = n_{(1)}^{eq}$ and $n = n_{(2)}^{eq}$ through such changes requires at least energy of order $16E_c$. This estimate is obtained using Fig. 7 as a maximum value of the red dashed curve. Moreover, the SET should go through several transitions $(n) \rightarrow (n-1)$ to reach the equilibrium state $n = n_{(1)}^{eq}$ from $n = n_{(2)}^{eq}$. Thus the probability of such a switching between equilibrium states is negligible.

For barrier $\Delta W_p \sim k_B T_{FE}$ the system switches between states $n = n_{(1)}^{eq}$ and $n = n_{(2)}^{eq}$. This behavior is shown in Fig. 8 where we depict functions $n(t)$ and $p(t)$ obtained using an MC simulation with the following parameters $\alpha_P = -0.15$, $e^2\tilde{\beta}_P = 0.2$, $C_g^0 = 0.002\,C_\Sigma$, and $Q_0 = 0$. Our MC simulations show that in this case there is no hysteresis behavior of the conductance as function of Q_0. This happens because the switching between different polarization states $p_{1,2}^{eq}|_n$ means that on the long-time scale the FE layer behaves as a paraelectric layer due to strong fluctuations. Note that such a mechanism of hysteresis suppression does not exist for
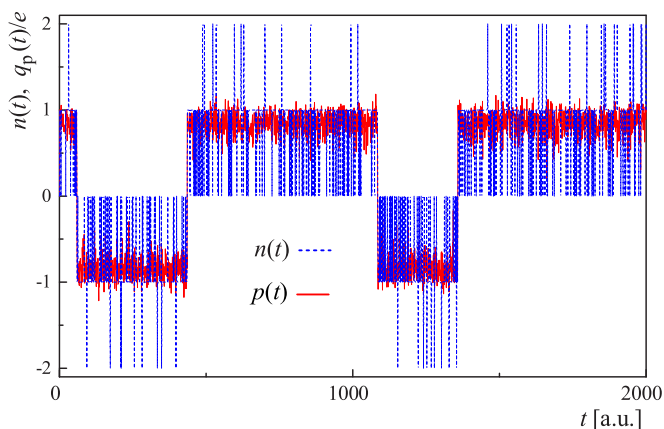
FIG. 8. (Color online) Island population n (blue dashed line) and FE layer induced charge, q_p/e, (red solid line) vs time t for the following parameters $\alpha_P = -0.15$, $e^2 \tilde{\beta}_P = 0.2$, $C_g^0 = 0.002\,C_\Sigma$, and $Q_0 = 0$. The FE layer polarization switches between two equilibrium states due to thermal fluctuations.

temperatures $T_C < T_{FE} < T_C^0$. In this region, the polarization p has always a single value. The suppression of hysteresis due to consecutive change of n is very improbable too. Therefore the conductance hysteresis is rather robust in the region $T_C < T_{FE} < T_C^0$, however, it is not very stable for $T_{FE} < T_C$.

D. SET with "slow" FE (dielectric) in the gate capacitor ($t_{FE} \gg t_{ex}$)

The characteristic time t_{ex} is the time between consecutive electron jumps to the grain. It depends on the gate voltage and it is comparable with t_d for weak Coulomb blockade.

The intermediate region, $t_d \ll t_{FE} \ll t_{ex}$, shows similar results for the conductance peak value as the region $t_{FE} \gg t_{ex}$. However, the peak shape in the intermediate region is quantitatively different since by changing the gate voltage V_g the ratio t_{FE}/t_{ex} changes too. However, our calculations show that the difference in the shape of the peaks is not qualitative. Therefore it is difficult to observe it in an experiment. Thus we consider both the intermediate and the "slow" FE regions simultaneously.

The limit of slow FE was studied before using the mean-field theory. In particular, two different situations were discussed in Refs. [24,27]. In Ref. [27], the SET with a linear dielectric material in the gate capacitor was discussed. It was shown that due to coupling of a fast SET system with a slow dielectric system, the hysteresis of the conductance as a function of Q_0 appears at a large positive susceptibility of the dielectric layer [$\chi_0 > \chi_0^{cr} = T_e\,C_\Sigma\,/(\pi\,C_g^0(E_c + T))$]. Reference [24] studied the SET with a strongly nonlinear FE material in the gate capacitor. Similar to the case of "fast" FE layer, the hysteresis in the vicinity of the point $Q_0 = 0$ was predicted. In the present paper, we study the conductance behavior moving from "fast" to "slow" FE (dielectric) in the presence of FE (dielectric) polarization fluctuations. These fluctuations substantially modify the behavior of SET even in the case of "slow" FE.

Following the mean-field theory of the SET with "slow" and weak dielectric layer ($0 < \chi_0 < \chi_0^{cr}$) [24] in the gate capacitor,

the conductance in the vicinity of $Q_0 = e/(2\epsilon_0)$ has the form

$$\sigma^{MF}/\sigma_0 \approx \frac{e\delta Q_0/(C_\Sigma\,k_B T_e)}{\sinh\left(e\delta Q_0/(C_\Sigma\,k_B T_e)\right)} \approx 1 - \frac{1}{6}\left(\frac{e\delta Q_0}{C_\Sigma\,k_B T_e}\right)^2,$$
(18)

where $\delta Q_0 = Q_0 - e/(2\epsilon_0)$. Equation (18) is valid for small deviations δQ_0. The FE fluctuations lead to averaging of the maximum over a finite region of Q_0. This region is proportional to the square root of the FE fluctuations dispersion, $S_g\sqrt{D_p} \sim \sqrt{T_{FE}}$. For equal temperatures $T_{FE} = T_e = T$, the averaging gives the following maximum value for the conductance:

$$\sigma_{max}^{av} = \sigma_0\left[1 - \frac{1}{18}\left(\frac{eS_g\sqrt{D_p}}{C_\Sigma\,k_B T}\right)^2\right]$$

$$= \sigma_0\left(1 - \frac{1}{18}\frac{4\pi C_g^0 e^2 \chi}{C_\Sigma^2\,k_B T}\right).$$
(19)

Equation (19) shows that the averaging over fluctuations leads to a decrease of the conductance peak value. Moreover, with decreasing the temperature, the conductance peak value decreases. This unexpected behavior is related to the fact that fluctuations of FE polarization behave as $\sqrt{T}$ leading to the "strong" $\sim\sqrt{T}$ free energy difference fluctuations. Below, we will show that FE fluctuations also smear the hysteresis appearance for $\chi_0 > \chi_0^{cr}$.

E. Transition from "fast" to "slow" FE (dielectric)

The analytical consideration is difficult for $t_{FE} \sim t_d$. Therefore we use MC simulations to study this region.

1. $T_{FE} > T_C^0$.

In the case of "fast" FE (dielectric), the conductance appears as a series of peaks as a function of the gate charge Q_0. Here, we consider the case of linear FE (dielectric) response. In this case, the period of peaks and height is constant and does not depend on Q_0. The peak height is defined by an effective additional Coulomb blockade. In the case of "slow" FE (dielectric), the conductance is also a periodic function of Q_0 (see Refs. [24,27]) with the same period as in the case of a "fast" dielectric. However, the shape of the conductance peaks strongly depends on the magnitude of the dielectric susceptibility, χ_0. For large susceptibility, the conductance shows a hysteresis behavior as a function of Q_0 while for small susceptibility the hysteresis is absent. The hysteresis behavior was demonstrated in Refs. [24,27] using the mean-field theory in the absence of fluctuations of the FE (dielectric) polarization. Our numerical simulations show that FE fluctuations destroy the hysteresis for temperatures $T_{FE} = T_e = T$. Lowering the FE temperature T_{FE} decreases the fluctuations of Q_0 but the hysteresis width also decreases with electronic temperature T_e. Therefore, to observe the hysteresis in the case of a "slow" dielectric, it is necessary to use the SET with different temperatures of the dielectric layer and the current conducting circuit, $T_{FE} < T_e$.

Figure 9 shows the evolution of function $\sigma(Q_0)$ with increasing parameter γ for large susceptibility χ_0 for the following parameters: $C_g^0 = 0.03\,C_\Sigma$, $\alpha_P = 0.5$, $e^2\tilde{\beta}_P = 3 \times 10^{-4}$, $T_e = 0.06E_c$. Panel (a) shows the ideal case in
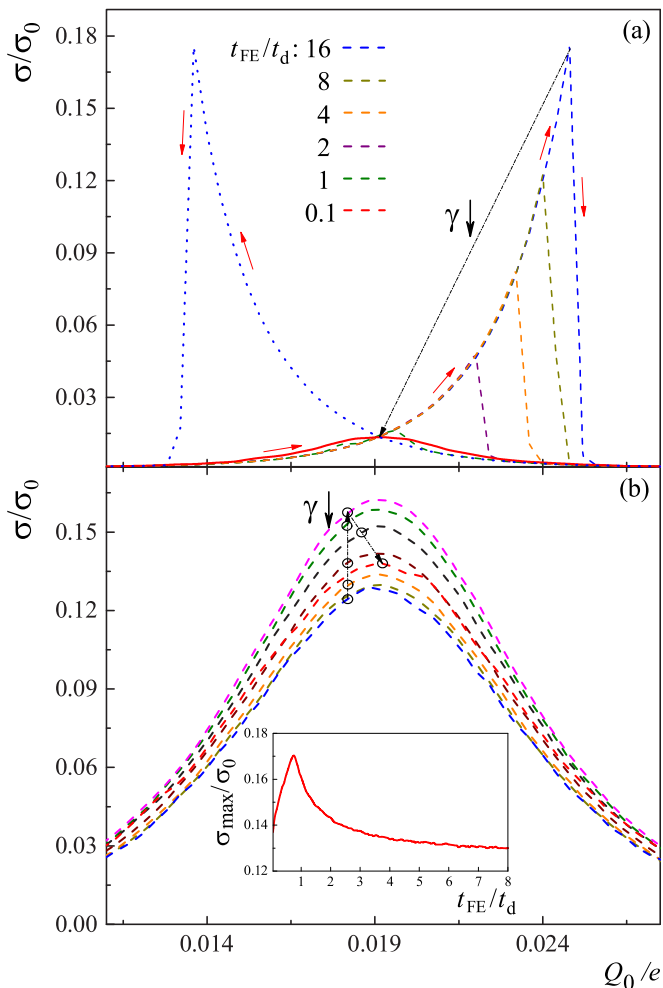
FIG. 9. (Color online) Conductance of SET as a function of Q_0 for different t_{FE}. (a) FE fluctuations are absent ($T_{FE} \ll T_e$). Red arrows show the path around the hysteresis loop. Both hysteresis branches are shown for $t_{FE}/t_d = 16$. (b) FE fluctuations are present ($T_{FE} = T_e$). The inset in the panel (b) shows the dependence of the peak value of the conductance on t_{FE}.

the absence of FE fluctuations and temperatures $T_{FE} \ll T_e$. For large FE relaxation time, $t_{FE} \gg t_d$, the hysteresis is very pronounced, see blue dashed and blue dotted lines. Red solid arrows show the path around the hysteresis loop. The hysteresis width and the maximum value of conductance decrease with decreasing time t_{FE} (γ). For $t_{FE} \ll t_d$, the hysteresis disappears and the conductance is suppressed due to an additional Coulomb blockade effect. The situation is very different for finite FE fluctuations and temperatures $T_{FE} = T_e$, see panel (b). In this case, the conductance hysteresis is absent for $t_{FE} \gg t_d$. The conductance as a function of Q_0 has a peak in the vicinity of $\epsilon_0 Q_0 = e/2$. The peak value has a nonmonotonic behavior with t_{FE}. The inset in panel (b) shows the conductance peak value, $\sigma_{max} = \sigma|_{\epsilon_0 Q_0 = e/2}$, as a function of t_{FE}. The curve has a peak at $t_{FE} \approx t_d$.

If susceptibility, χ_0, is small and the hysteresis is absent at $t_{FE} \gg t_d$, the conductance is a periodic function of Q_0 [in the absence of nonlinear term in Eq. (4)]. Figure 10 shows the dependence of the peak value of the conductance, $\sigma_{max} = \sigma|_{\epsilon_0 Q_0 = e/2}$, on the FE relaxation time, t_{FE}. The curves
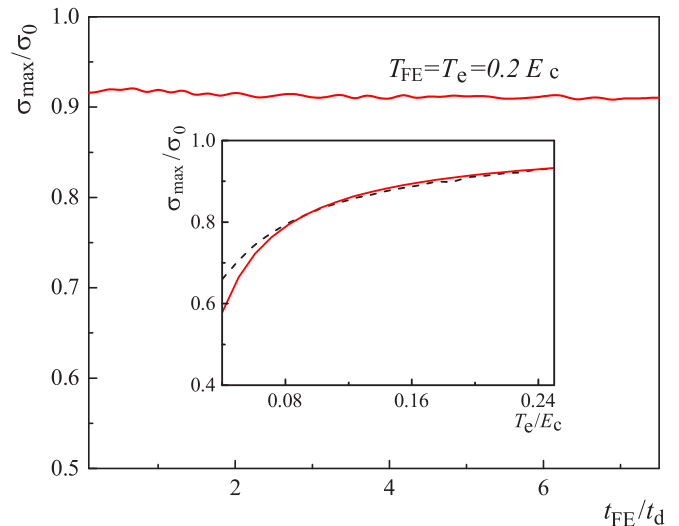

FIG. 10. (Color online) Conductance peak value vs t_{FE} for small FE (dielectric) susceptibility, χ_0. The inset shows the conductance peak value at $t_{FE}/t_d = 8$ as a function of temperature $T_e = T_{FE}$. The dashed black line shows the result of MC simulations. The red solid line corresponds to the modified Eq. (19).

in Fig. 10 are plotted in the presence of FE fluctuations for the following parameters: $\alpha_P = 2$, $C_g^0 = 0.01 C_\Sigma$, $T_e = T_{FE} = 0.2 E_c$. One can see that in this case the peak value does not depend on the FE relaxation time t_{FE}. The inset in Fig. 10 shows the dependence of the conductance peak value on temperature for time $t_{FE} \gg t_d$, see the black dashed line. The peak value increases with temperature. It is in a qualitative agreement with Eq. (19). The red line in the inset shows the same function as in Eq. (19), however, with a different coefficient $(1/7)$ instead of $(1/18)$. All curves in the inset are plotted for fixed susceptibility, χ_0.

2. $T_{FE} < T_C^0$.

Above, we have shown that for "fast" FE, the conductance has hysteresis as a function of Q_0. Our MC simulations show that this hysteresis exists even for "slow" FE. The hysteresis is robust against the FE fluctuations (see red and black lines in the inset in Fig. 11). The inset in Fig. 11 shows the SET conductance versus the gate charge Q_0 and the FE relaxation time t_{FE} in the presence of FE polarization fluctuations for the following parameters: $C_g^0 = 0.2 C_\Sigma$ and $T_e = T_{FE} = 0.2 E_c$, $\alpha_P = -2$, $e^2 \tilde{\beta}_P = 0.13$. The conductance peak value decreases with increasing the FE relaxation time (see the curve in Fig. 11).

F. Discussion of some experimental problems

The important question about an implementation of the SET with an FE layer in the gate capacitor is related to the FE Curie temperature. This temperature and the dielectric permittivity decrease with decreasing FE layer thickness [48,49]. A critical thickness exists for most of FE materials. Below this thickness, the FE phase transition does not exist (T_C^0 becomes negative). Moreover, the boundary conditions at the FE layer surface in the SET also contribute to the degradation of FE properties. Since the grain voltage is not fixed, the FE internal electric field
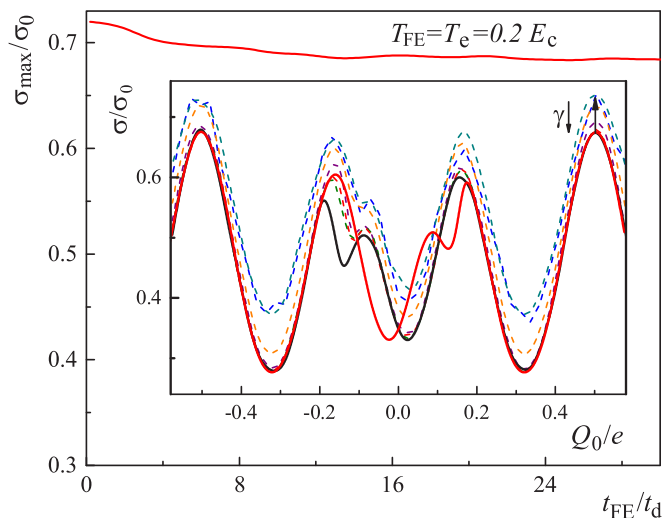
FIG. 11. (Color online) Conductance, $\sigma_{\max} = \sigma|_{Q_0=e/2}$, vs t_{FE} for negative susceptibility, χ_0, ($T_{\mathrm{e}} = T_{\mathrm{FE}} < T_C^0$). Inset: conductance of SET as a function of Q_0 for different t_{FE}. Red solid curve stands for increasing Q_0. All other curves stand for decreasing Q_0. Solid red and black lines are for $t_{\mathrm{FE}} \gg t_{\mathrm{d}}$. Blue dashed line shows the opposite case, $t_{\mathrm{FE}}/t_{\mathrm{d}} = 0.1$. All other curves correspond to intermediate t_{FE}.

is not screened effectively leading to the reduction of the FE temperature and dielectric permittivity. The question about the electric properties of an FE material confined in such a small volume is currently open. In our consideration, we assume FEs with low Curie temperature. One example is the TTF-CA FE material. Bulk TTF-CA under close circuit boundary conditions has a Curie temperature $T_C^0 = 80$ K [46,50]. For this FE material, T_C^0 can be of order of $(0.1 - 0.2)E_c$. In Ref. [51], a TTF-CA film was confined at one surface with a granular film. Therefore there was no effective screening of the internal FE field. In this system, the FE Curie temperature has a lower value $T_C^0 = 50$ K.

For Coulomb blockade effects to exist at such a high temperature (~ 50 K), it is necessary to produce a rather small island in the SET with a size of approximately 5 nm. Assuming that the insulator thickness in the tunnel junctions is about 1 nm and $\epsilon_{\mathrm{jun}} \approx 5$, we find $C \sim 10^{-18}$ F. Usually, the resistance of the tunneling junction is about 10^6 Ohm leading to the discharging time $t_{\mathrm{d}} \sim 10^{-12}$ s. Using tunnel junctions with resistance $\sim 10^7$ Ohm, one can increase the FE discharging time to $t_{\mathrm{d}} \sim 10^{-11}$ s.

It is known that the dielectric relaxation time in materials depends on the mechanism of dielectric response. Two groups of materials are most promising for our purposes. In the first group, the dielectric response is caused by the elastic mechanisms. The electronic mechanism does not produce a very high dielectric permittivity, instead it gives a very fast response with $t_{\mathrm{FE}} \sim 10^{-15}$ s. Usual insulators such as Si, SiO$_2$, and Al$_2$O$_3$ have such a response mechanism. These materials can not be used as "retarded" in an SET. An SET with these insulators can be described using "classical" theory. The ionic elastic mechanism gives a higher dielectric permittivity but slower response with $t_{\mathrm{FE}} \sim 10^{-11}-10^{-14}$ s. This mechanism substantially contributes to the dielectric response of semiconductors (GaAs and CdS) and ionic crystals

such as NaCl. Insulators with this type of dielectric response can be used to investigate the limits $t_{\mathrm{FE}} \ll t_{\mathrm{d}}$ and $t_{\mathrm{FE}} \sim t_{\mathrm{d}}$. A second group of materials have thermal mechanisms of dielectric response. These mechanisms give a rather high permittivity but longer relaxation time, $t_{\mathrm{FE}} \sim 10^{-4}-10^{-10}$ s. Moreover, the relaxation time in these materials increases with decreasing temperature. The dielectric response of relaxor FEs (such as PMN-PSN [52] with $t_{\mathrm{FE}} \sim 10^{-9}$ s at room temperature) are usually due to a thermal mechanism. These materials can be considered as slow FEs with $t_{\mathrm{FE}} \gg t_{\mathrm{d}}$.

Most FEs materials are rather slow with a dielectric relaxation time well below 1 THz. This is due to the ionic nature of their dielectric response. However, recently, new types of electronic FEs were discovered. One of them is TTF-CA. This material has dielectric relaxation time in the terahertz region [47]. This material can be used to study the interaction of an SET with retarded FEs.

IV. CONCLUSION

We studied the SET with an FE or a dielectric placed in the gate capacitor. In contrast to the previous papers, we investigated the system behavior for an arbitrary ratio between the FE relaxation time, t_{FE}, and the SET characteristic time t_{d}. We used analytical methods and Monte Carlo simulations to study the SET behavior.

We considered the case of "fast" FE (dielectric) with $\hbar/E_c \ll t_{\mathrm{FE}} \ll t_{\mathrm{d}}$. We showed that this case is different from the "classical" SET theory, where the instant response, $\hbar/E_c \gg t_{\mathrm{FE}}$, of a dielectric material is assumed. Thus a "fast" FE has a retarded response. We showed that a retarded FE (dielectric) response leads to the appearance of an additional contribution to the Coulomb blockade effect and suppresses the SET conductance. The conductance as a function of the gate charge Q_0 behaves differently at different temperatures. Below a certain temperature T_C^0 (which is the Curie temperature of the FE inside the gate capacitor), the conductance shows the hysteresis behavior. Above T_C^0, no hysteresis appears in the case of "fast" FE. Monte Carlo simulations allowed us to take into account fluctuations of the FE (dielectric) polarization. For "fast" FE, these fluctuations partially suppress the additional Coulomb blockade effect. We showed that conductance hysteresis is robust against these fluctuations.

We studied the case of a "slow" FE (dielectric), $t_{\mathrm{FE}} \gg t_{\mathrm{d}}$. This limit was discussed in literature using the mean-field approach in the past. An interesting feature is related to the fact that due to the coupling of a fast SET subsystem with a slow FE subsystem the conductance of the SET showed a hysteresis behavior even for temperatures $T > T_C^0$. Thus the nature of the hysteresis is not related to the spontaneous polarization of the FE layer and may appear even with a simple dielectric being placed in the gate capacitor. We used Monte Carlo simulations to reinvestigate this case. We found that FE (dielectric) fluctuations suppress the hysteresis. The only way to observe this hysteresis is to produce an FE (dielectric) layer temperature lower than the temperature of electrons in the SET leads (source and drain) and the island ($T_{\mathrm{FE}} \ll T_{\mathrm{e}}$).

We showed that for "slow" FE and low temperature, $T < T_C^0$, the SET conductance as a function of the gate charge Q_0

shows a hysteresis due to FE instability. This hysteresis is robust against FE fluctuations.

Using the Monte Carlo simulations, we studied the transitional region between "fast" and "slow" FE. The transition depends on the temperature [or the susceptibility of the FE (dielectric) layer]. At high temperatures (low susceptibility), the peak value of the SET conductance is almost independent of the FE relaxation time. For temperatures close to T_C^0 (high susceptibility), the conductance peak value nonmonotonically depends on the FE relaxation time. A maximum appears close to $t_{FE} = t_d$. Below the Curie point ($T < T_C^0$), the conductance peak value decreases with increasing t_{FE}.

[1] F. Giazotto, Nat. Phys. **11**, 527 (2015).

[2] D. J. van Woerkom, A. Geresdi, and L. P. Kouwenhoven, Nat. Phys. **11**, 547 (2015).

[3] Z.-Z. Li, C.-H. Lam, and J. Q. You, Sci. Rep. **5**, 11416 (2015).

[4] I. M. Khaimovich, J. V. Koski, O. P. Saira, V. E. Kravtsov, and J. P. Pekola, Nat. Commun. **6**, 7010 (2015).

[5] K. Horibe, T. Kodera, and S. Oda, Appl. Phys. Lett. **106**, 053119 (2015).

[6] M. R. Islam, D. Joung, and S. I. Khondaker, Nanoscale **7**, 9786 (2015).

[7] P. Hakkinen, A. Isacsson, A. Savin, J. Sulkko, and P. Hakkonen, Nano Lett. **15**, 1667 (2015).

[8] P. Strasberg, G. Schaller, T. Brandes, and M. Esposito, Phys. Rev. Lett. **110**, 040601 (2013).

[9] A. V. Feshchenko, J. V. Koski, and J. P. Pekola, Phys. Rev. B **90**, 201407(R) (2014).

[10] P. G. Kirton and A. D. Armour, Phys. Rev. B **87**, 155407 (2013).

[11] K. K. Likharev, N. S. Bakhvalov, G. S. Kazacha, and S. I. Serdyukova, IEEE Trans. Magn. **25**, 1436 (1989).

[12] D. V. Averin and K. K. Likharev, J. Low Temp. Phys. **62**, 345 (1986).

[13] L. Y. Gorelik, A. Isacsson, M. V. Voinova, B. Kasemo, R. I. Shekhter, and M. Jonson, Phys. Rev. Lett. **80**, 4526 (1998).

[14] A. D. Armour and A. MacKinnon, Phys. Rev. B **66**, 035333 (2002).

[15] T. Nord, L. Y. Gorelik, R. I. Shekhter, and M. Jonson, Phys. Rev. B **65**, 165312 (2002).

[16] T. Novotny, A. Donarini, and A.-P. Jauho, Phys. Rev. Lett. **90**, 256801 (2003).

[17] N. M. Chtchelkatchev, W. Belzig, and C. Bruder, Phys. Rev. B **70**, 193305 (2004).

[18] A. D. Armour, M. P. Blencowe, and Y. Zhang, Phys. Rev. B **69**, 125313 (2004).

[19] A. D. Armour, Phys. Rev. B **70**, 165315 (2004).

[20] D. A. Rodrigues, J. Imbers, and A. D. Armour, Phys. Rev. Lett. **98**, 067204 (2007).

[21] C. B. Doiron, W. Belzig, and C. Bruder, Phys. Rev. B **74**, 205336 (2006).

[22] R. Hussein, A. Metelmann, P. Zedler, and T. Brandes, Phys. Rev. B **82**, 165406 (2010).

[23] S. A. Fedorov, A. E. Korolkov, N. M. Chtchelkatchev, O. G. Udalov, and I. S. Beloborodov, Phys. Rev. B **90**, 195111 (2014).

[24] S. A. Fedorov, A. E. Korolkov, N. M. Chtchelkatchev, O. G. Udalov, and I. S. Beloborodov, Phys. Rev. B **89**, 155410 (2014).

[25] J. P. Pekola, J. J. Vartiainen, M. Mottonen, O.-P. Saira, M. Meschke, and D. V. Averin, Nat. Phys. **4**, 120 (2014).

[26] B. A. Strukov and A. P. Levanyuk, *Ferroelectric Phenomena in Crystals* (Springer, Geidelberg, 1998).

[27] S. A. Fedorov, N. M. Chtchelkatchev, O. G. Udalov, and I. S. Beloborodov, Phys. Rev. B **92**, 115425 (2015).

[28] L. R. C. Fonseca, A. N. Korotkov, K. K. Likharev, and A. A. Odintsov, J. Appl. Phys. **78**, 3238 (1995).

[29] H.-S. Goan, Phys. Rev. B **70**, 075305 (2004).

[30] D. Mozyrsky, I. Martin, and M. B. Hastings, Phys. Rev. Lett. **92**, 018303 (2004).

[31] C. Waahuber and H. Kosina, IEEE Trans. Comp. **16**, 937 (1997).

[32] J. Bylander, T. Duty, and P. Delsing, Nature (London) **434**, 361 (2005).

[33] F. Giazotto, T. T. Heikkila, A. Luukanen, A. M. Savin, and J. P. Pekola, Rev. Mod. Phys. **78**, 217 (2006).

[34] A. N. Korotkov, M. R. Samuelsen, and S. A. Vasenko, J. Appl. Phys. **76**, 3623 (1994).

[35] O.-P. Saira, M. Meschke, F. Giazotto, A. M. Savin, M. Möttönen, and J. P. Pekola, Phys. Rev. Lett. **99**, 027203 (2007).

[36] S. Lefevre, S. Volz, and P.-O. Chapuis, Int. J. Heat Mass Transf. **49**, 251 (2006).

[37] K. L. Grosse, M.-H. Bae, F. Lian, E. Pop, and W. P. King, Nat. Nanotechnol. **6**, 287 (2011).

[38] J. B. Khurgin, Phys. Rev. Lett. **98**, 177401 (2007).

[39] Y.-S. Liu, B. C. Hsu, and Y.-C. Chen, J. Phys. Chem. C **115**, 6111 (2011).

[40] L. D. Landau and E. Lifshitz, *Course of Theoretical Physics: Vol. 8: Electrodynamics of Continuous Media* (Pergamon Press, Bristol, 1960).

[41] R. Zwanzig, J. Stat. Phys. **9**, 215 (1973).

[42] M. Bixon and R. Zwanzig, J. Stat. Phys. **3**, 245 (1971).

[43] M. H. Devoret, D. Esteve, H. Grabert, G. L. Ingold, H. Pothier, and C. Urbina, Phys. Rev. Lett. **64**, 1824 (1990).

[44] S. M. Girvin, L. I. Glazman, M. Jonson, D. R. Penn, and M. D. Stiles, Phys. Rev. Lett. **64**, 3183 (1990).

[45] M. Devoret and H. Grabert, *Single Charge Tunneling*, (New York, Plenum, 1992), Vol. 264.

[46] K. Kobayashi, S. Horiuchi, R. Kumai, F. Kagawa, Y. Murakami, and Y. Tokura, Phys. Rev. Lett. **108**, 237601 (2012).

[47] T. Miyamoto, H. Yada, H. Yamakawa, and H. Okamoto, Nat. Commun. **4**, 2586 (2013).

[48] V. M. Fridkin, Phys. Usp. **49**, 193 (2006).

[49] V. M. Fridkin, R. V. Gaynutdinov, and S. Ducharme, Phys. Usp. **53**, 199 (2010).

[50] M. Buron-LeCointe, M. H. Lemee-Cailleau, H. Cailleau, S. Ravy, J. F. Berar, S. Rouziere, E. Elkaim, and E. Collet, Phys. Rev. Lett. **96**, 205503 (2006).

[51] M. Huth, A. Rippert, R. Sachser, and L. Keller, Mater. Res. Express **1**, 046303 (2014).

[52] R. Grigalaitis, J. Banys, J. Macutkevic, R. Adomavicius, A. Krotkus, K. Bormanis, and A. Sternberg, J. Eur. Ceram. Soc. **30**, 613 (2010).